International Journal of Mechanical, Industrial and Aerospace Sciences
ISSN: 2517-9950
Vol:11, No:5, 2017

Modeling the Effect of Thermal Gradation on Steady-State Creep Behavior of Isotropic Rotating Disc Made of Functionally Graded Material

Tania Bose, Minto Rattan, Neeraj Chamoli

Abstract—In this paper, an attempt has been made to study the effect of thermal gradation on the steady-state creep behavior of rotating isotropic disc made of functionally graded material using threshold stress based Sherby's creep law. The composite discs made of aluminum matrix reinforced with silicon carbide particulate have been taken for analysis. The stress and strain rate distributions have been calculated for the discs rotating at elevated temperatures having thermal gradation. The material parameters of creep vary radially and have been estimated by regression fit of the available experimental data. Investigations for discs made up of linearly increasing particle content operating under linearly decreasing temperature from inner to outer radii have been done using von Mises' yield criterion. The results are displayed and compared graphically in designer friendly format for the above said disc profile with the disc made of particle reinforced composite operating under uniform temperature profile. It is observed that radial and tangential stresses show minor variation and the strain rates vary significantly in the presence of thermal gradation as compared to disc having uniform temperature.

Keywords—Creep, functionally graded isotropic material, steady-state, thermal gradation.

I. Introduction

FUNCTIONALLY graded materials (FGMs) possess a number of advantages that make them attractive in potential applications, including a potential reduction of in-plane and transverse through-the-thickness stresses, an improved residual stress distribution, enhanced thermal properties, higher fracture toughness, and reduced stress intensity factors [3]. FGMs are usually associated with particulate composites where the volume fraction of particles varies in one or several directions. One of the advantages of a monotonous variation of volume fraction of constituent phases is the elimination of stress discontinuity that is often encountered in laminated composites and accordingly, avoiding delamination related problems [3]. Many commercial applications of FGM were proposed in 1984 by material scientists in the Sendai area of Japan as a means of preparing thermal barrier materials [18]. Some of the applications are machining tool, optical fiber, optical filter, surface material for wristwatch, blade of electric shaver, spike for baseball shoes, etc. Suryanarayanan et al. [17] studied the potential use of Al-SiC metal matrix composite with particular reference to the aerospace industry. Metal matrix composites were recommended as possible replacements for aluminium and it was seen that the exact set of properties depend on certain factors. Therefore, the factors such as reactivity at the interface, volume fraction of the reinforcing material, type of the reinforced materials and distribution of the reinforcing material were reviewed using the existing literature. The above said paper advocated the use of $Al - SiC$ metal matrix composite in the fuselage skins of high performance aircrafts. Hirai and Chen [9] described findings on the design, process and characteristics of FGM. Many fabrication processes have been developed, and various new materials with unique properties have been prepared by introducing graded structures. Gupta et al. [7] investigated the creep behavior of a rotating disc made of isotropic FGM having thermal gradient in the radial direction using Sherby's law. The analysis indicated that for the assumed linear particle distribution, the steady-state strain rates are significantly lower compared to that in an isotropic disc with uniform particle distribution. Durodola and Attia [5] explored the potential benefits of using fibre-reinforced, functionally graded materials for rotating hollow and solid disks. Several forms of gradation with the same nominal volume fraction of reinforcement were considered. The finite element method and direct numerical integration of the governing differential equations were used to predict stress and deformation distribution in the disks. Park *et al.* [12] studied the effect of stress on the creep properties of 30 vol.% silicon carbide particulate reinforced 6061 aluminium ($SiC_p - 6061Al$), produced by powder metallurgy in the temperature range of 618-678K. Rattan et al. [13] investigated the effect of stress exponent on steady state creep in an isotropic rotating disc made of aluminium silicon-carbide particulate ($Al - SiC_p$) composite. The creep behaviour has been described by Sherby's model and the analysis of steady state creep was carried out using von Mises' yield criterion. The stress and strain rate distributions developed due to rotation have been calculated and the study revealed that the stress exponent of 8 gave better approximation to experimental results than those of 3 and 5. Further, Rattan et al. [14] investigated the creep response for isotropic axisymmetric rotating disc made of particle-reinforced FGM. The results obtained for non linear variation of particle distribution along the radial distance of the disc were compared with that of discs containing the same amount of particle distributed uniformly or linearly along the radial distance. It was observed that a

The authors acknowledge the grant (F. No. 09/135(0706)/2014-EMR-I) received from Council of Scientific & Industrial Research Human Resource Development Group, New Delhi, India.

Minto Rattan is Assistant Professor in the Department of Applied Science, University Institute of Engineering and Technology, Panjab University, Chandigarh, India.

N. Chamoli is Assistant Professor in the Department of Mathematics, D.A.V. College, Chandigarh, India (e-mail: neeraj_chamoli@yahoo.com).

functionally graded rotating disc with parabolic profile can be more efficient than those with uniform distribution or linear variations of particle. FGMs have high potential for applications in components subjected to severe mechanical and thermal loadings because of their unique performance due to spatial tailoring of properties at a microscopic level [16]. Ahmadi and Eskandari [1] addressed the asymmetric problem of rocking rotation of a circular rigid disk embedded in a finite depth of a transversely isotropic half-space. The results related to contact stress distribution across the disk region and the equivalent rocking stiffness of the system were expressed in terms of solution of Fredholm integral equation. The effects of anisotropy on the rocking stiffness factor were also discussed in details.

Keeping in view the work done in the past, this paper throws light on the steady state creep behavior of rotating disc made of linearly varying functionally graded material under the effect of linear thermal gradation. A comparative study has been carried out to find stress and strain rate distributions for discs operating under uniform temperature and linear thermal gradients.

II. Mathematical Modeling

A. Disc Profile

We have considered functionally graded rotating disc made of aluminium matrix reinforced with silicon-carbide particles $Al-SiC_p$, having inner radius $(a = 0.03175m)$ and outer radius $(b = 0.1524m)$, as taken by Wahl [19]. The reinforced silicon carbide particles vary linearly from the inner to outer radius; as a result, the density and the creep parameters will vary along the radial distance. Thus the material properties of the disc are assumed to be functions of the volume fraction of the constituent materials. The particle content $(vol.\%)$ of SiC_p at any radius r, which is designated as $V(r)$, vary linearly as:

$$V(r) = A - Br, \qquad a \le r \le b \tag{1}$$

where

$$A = \frac{bV_{max} - aV_{min}}{b-a} \tag{2}$$

and

$$B = \frac{V_{max} - V_{min}}{b-a} \tag{3}$$

where $V_{min} = 10\ vol.\%$ and $V_{max} = 35.59\ vol.\%$ are taken as the particle content at the inner radius and outer radius, respectively.

Using the law of mixture, the density variation in the composite disc along the radial distance is expressed as

$$\rho(r) = \rho_m + (\rho_d - \rho_m)\frac{V(r)}{100} \tag{4}$$

where $\rho_m = 2713kg/m^3$ and $\rho_d = 3210kg/m^3$ are the densities of the matrix alloy and of the dispersed silicon carbide particles, respectively [4], [10]). From (1) and (4), we have

$$\rho(r) = \rho_m + (\rho_d - \rho_m)\frac{A - Br}{100} \tag{5}$$

TABLE I
Description of Discs Investigated

Disc	Profile	Temperature (K)			Temperature Gradient (K)
		T_a	T_b	T_{avg}	$T_b - T_a$
D_1	uniform	623	623	623	0
D_2	linear	638	613.37	623	24.63
D_3		653	603.75	623	49.25
D_4		668	594.13	623	73.87

If the average particle content in the FGM disc is $V_{avg} = 20\ vol.\%$, and h is the uniform thickness of the disc, then

$$\int_a^b 2\pi r h V(r) dr = V_{avg}.\pi\ h(b^2 - a^2) \tag{6}$$

From (1) and (6), we get the following relation:

$$V_{avg} = A - \frac{2}{3}\frac{B(b^3 - a^3)}{(b^2 - a^2)} \tag{7}$$

B. Temperature Profile

For the present study, the FGM discs with following temperature profiles have been considered;

(i) Disc D_1 operating at *uniform temperature* of $623K$ along the radial distance.

(ii) Discs D_2, D_3 and D_4 operating at *linearly decreasing* thermal gradient have temperature distribution, T_r given as:

$$T_r = A - Br, \qquad a \le r \le b \tag{8}$$

where

$$A = \frac{bT_a - aT_b}{b-a} \tag{9}$$

and

$$B = \frac{T_a - T_b}{b-a} \tag{10}$$

Here T_a and T_b are the imposed temperatures at the inner radius a and outer radius b respectively. The values of T_a and T_b for discs D_2, D_3 and D_4 are given in Table I.

C. Creep Parameters

Sherbys' law [15] is used to describe the steady-state creep response of the $Al-SiC_p$ FGM disc given by:

$$\dot{\bar{\epsilon}} = [M(\bar{\sigma} - \sigma_0)]^8 \tag{11}$$

where the symbols $\dot{\bar{\epsilon}}$, $\bar{\sigma}$, σ_0 denote the effective strain rate under biaxial stress, the effective stress under biaxial stress, threshold stress respectively, and the creep parameter M is given by:

$$M = \frac{1}{E}\left[\frac{AD_L\lambda^3}{|\vec{b_r}|^5}\right]^{1/8} \tag{12}$$

where the symbols A, D_L, λ, E, $|\vec{b_r}|$ denote, respectively, constant sensitive to microstructure, lattice diffusivity, subgrain size, Young's modulus of elasticity and magnitude of burgers vector.

The creep parameters M and σ_0 as given by (11) depend on the type of material and are also affected by the operating temperature T. In a composite material, the particle size (p) and the particle content $(V(r))$ are the primary material

TABLE II
MATERIAL PARAMETERS OBTAINED FROM EXPERIMENTAL DATA OF PANDEY ET AL. [11]

Particle size p (μm)	Temperature T (K)	Particle content V $(vol.\%)$	Creep parameters M $(s^{-1/8}MPa)$	σ_0 (MPa)
1.7	623	10	0.00963	15.24
14.5			0.01444	11.46
45.9			0.01897	13.65
1.7	623	10	0.00963	15.24
		20	0.00594	24.83
		30	0.00518	34.32
1.7	623	20	0.00594	24.83
	673		0.00897	24.74
	723		0.01295	25.72

variables influencing these parameters. The value of M and σ_0 have been obtained from the creep results reported for $Al-SiC_p$ composite by Pandey et al. [11] and are shown in Table II.

A regression analysis has been performed using Data Fit software. In the analysis, variables $M(r)$ and $\sigma_0(r)$ are depending on p, $V(r)$ and $T(r)$ and the developed regression equations are given as:

$$\ln(M(r)) = 0.211ln(p)+4.89ln(T(r))-0.59ln(V(r))-34.91 \quad (13)$$

$$\sigma_0(r) = -0.0205(p) + 0.037(T(r)) + 1.033(V(r)) - 4.969 \quad (14)$$

D. Mathematical Formulation

From symmetry considerations, principal stresses are in the radial, tangential and axial directions for the disc rotating with angular velocity ω. For the purpose of modeling, the following assumptions are made:

(a) Steady state condition of stress.
(b) Elastic deformations neglected as compared to the creep deformations.
(c) Biaxial state of stress exists at each point of the disc.
(d) The disc is fitted on a splined shaft where small axial movement is permitted.

Taking reference frame along the directions r, θ and z, the generalized constitutive equations for creep in an isotropic rotating disc are given by:

$$\dot{\epsilon}_r = \frac{\dot{\bar{\epsilon}}}{2\bar{\sigma}}[2\sigma_r - (\sigma_\theta + \sigma_z)] \quad (15)$$

$$\dot{\epsilon}_\theta = \frac{\dot{\bar{\epsilon}}}{2\bar{\sigma}}[2\sigma_\theta - (\sigma_z + \sigma_r)] \quad (16)$$

$$\dot{\epsilon}_z = \frac{\dot{\bar{\epsilon}}}{2\bar{\sigma}}[2\sigma_z - (\sigma_r + \sigma_\theta)] \quad (17)$$

where the effective stress using von Mises' yield criterion is given by:

$$\bar{\sigma} = \frac{1}{\sqrt{2}}[(\sigma_r - \sigma_\theta)^2 + (\sigma_\theta - \sigma_z)^2 + (\sigma_r - \sigma_z)^2]^{1/2} \quad (18)$$

and $\dot{\epsilon}_r$, $\dot{\epsilon}_\theta$, $\dot{\epsilon}_z$ and σ_r, σ_θ, σ_z are the strain rates and stresses respectively in the directions indicated by the subscripts and $\dot{\bar{\epsilon}}$ is the effective strain rate. For biaxial state of stress ($\sigma_z = 0$) and the constitutive equations are

$$\dot{\epsilon}_r = \frac{d\dot{u}_r}{dr} = \frac{[M(r)(\bar{\sigma} - \sigma_0(r))]^8(2x-1)}{2(x^2-x+1)^{1/2}} \quad (19)$$

$$\dot{\epsilon}_\theta = \frac{\dot{u}_r}{r} = \frac{[M(r)(\bar{\sigma} - \sigma_0(r))]^8(2-x)}{2(x^2-x+1)^{1/2}} \quad (20)$$

$$\dot{\epsilon}_z = -(\dot{\epsilon}_r + \dot{\epsilon}_\theta) \quad (21)$$

where $x = \frac{\sigma_r(r)}{\sigma_\theta(r)}$ is the ratio of radial and tangential stress at any radius r and u_r is the radial displacement.

The equation of motion for a rotating disc of uniform thickness h may be obtained by considering the equilibrium of an element in the composite disc confined between radial distances r and $r+dr$ and an interval of angle between θ and $\theta+d\theta$. The equilibrium of forces in the radial direction of the element implies that

$$\frac{d}{dr}[r\sigma_r(r)] - \sigma_\theta(r) + \rho(r)\omega^2 r^2 = 0 \quad (22)$$

where ρ is the density of the composite.

Equations (19) and (20) can be solved to obtain $\sigma_\theta(r)$ as given below:

$$\sigma_\theta(r) = \frac{(\dot{u}_a)^{1/8}}{M(r)}\psi_1(r) + \psi_2(r) \quad (23)$$

where

$$\psi_1(r) = \frac{\psi(r)}{(x^2-x+1)^{1/2}}, \quad (24)$$

$$\psi_2(r) = \frac{\sigma_0(r)}{(x^2-x+1)^{1/2}}, \quad (25)$$

$$\psi(r) = \left[\frac{2(x^2-x+1)^{1/2}}{r(2-x)} exp \int_a^r \frac{\phi(r)}{r} dr\right]^{1/8}, \quad (26)$$

and

$$\phi(r) = \frac{(2x-1)}{(2-x)}. \quad (27)$$

Knowing the tangential stress distribution $\sigma_\theta(r)$, values of $\sigma_r(r)$ can be obtained from (22) as follows:

$$\sigma_r(r) = \frac{1}{r}\int_a^r \sigma_\theta(r)dr - \frac{\omega^2}{r}[X-Y]. \quad (28)$$

where,

$$X = \frac{(r^3-a^3)}{3}\left(\rho_m + (\rho_d - \rho_m)\frac{A}{100}\right) \quad (29)$$

and

$$Y = \frac{(\rho_d - \rho_m)}{100}\frac{B(r^4-a^4)}{4} \quad (30)$$

As the tangential stress, σ_θ , and the radial stress, σ_r, are determined by (23) and (28) at any point within the composite disc, the strain rates $\dot{\epsilon}_r$, $\dot{\epsilon}_\theta$ and $\dot{\epsilon}_z$ are calculated from (19), (20) and (21) respectively.

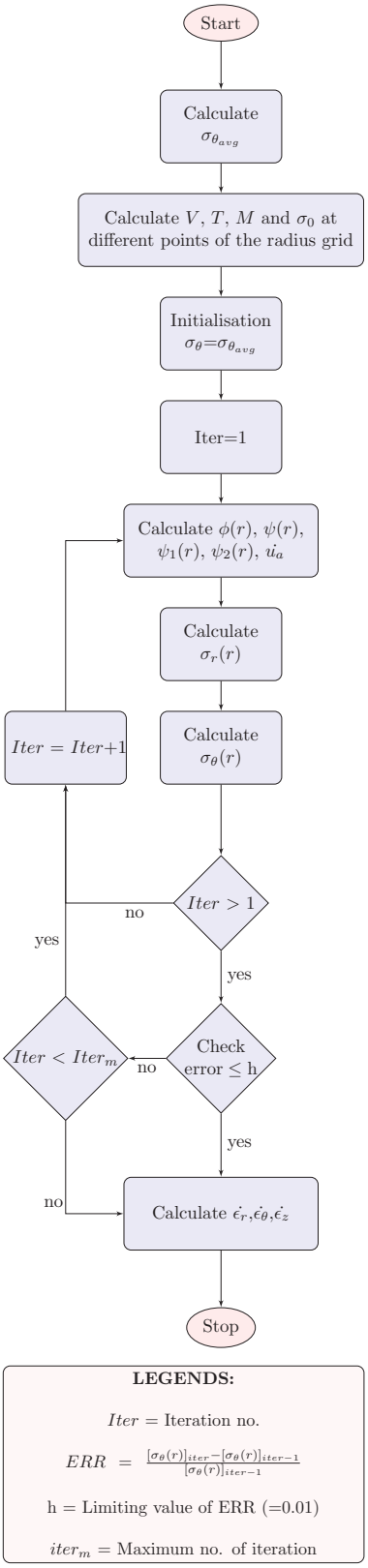

Fig. 1 Numerical scheme of computation

TABLE III
TYPES OF DISC AND OPERATING CONDITIONS OF THE DISC

Type of disc		Particle content $(vol.\%)$			Particle size (μm)
		V_{max}	V_{min}	V_{avg}	p
FGM Disc	D_1	10	35.59	20	1.7
FGM Disc	D_2	10	35.59	20	1.7
FGM Disc	D_3	10	35.59	20	1.7
FGM Disc	D_4	10	35.59	20	1.7

TABLE IV
VALUES USED BY WAHL ET AL. [19] DURING EXPERIMENT

Parameters for steel disc:-		
Density of disc material,	ρ	7823.18 kg/m^3
Inner radius of the disc,	a	0.03175 m
Outer radius of the disc,	b	0.1524 m
Creep parameter,	M	$4.72 \times 10^{-4}(s^{-\frac{1}{8}}/MPa)$
Creep parameter,	σ_0	-54.05 MPa
Operating conditions:-		
Angular velocity,	ω	15000 r/min
Operating Temperature,	T	810.78 K
Creep duration,	t	180 hr

E. Numerical Computation

The stress distribution is evaluated from the above analysis by iterative numerical scheme of computations as given in Figure1.

The iterations are continued till the process converges, yielding the values of stresses at different points of the radius grid. An iterative solution technique can be employed until the boundary conditions $\sigma_r(a) = 0$ and $\sigma_r(b) = 0$ are satisfied [2], [6]. For rapid convergence, as Gupta et al. [8] has done, 75% of the value of $\sigma_\theta(r)$ obtained in the current iteration has been mixed with 25% of the value of $\sigma_\theta(r)$ obtained in the last iteration for the use in the next iteration, i.e.

$$\sigma_{\theta_{next}} = 0.25\ \sigma_{\theta_{previous}} + 0.75\ \sigma_{\theta_{current}}. \qquad (31)$$

Based on the above mathematical formulation, a computer code in MATLAB has been generated to calculate the steady-state creep behavior of the disc having linearly decreasing particle content which is also subjected to thermal gradient. Numerical calculation has been done to obtain the steady-state creep response of the discs having particle size and particle content as shown in Table III.

F. Validation of the developed Computer Program

In order to validate the analysis and the developed computer program, the results for a rotating steel disc were obtained and compared with the available experimental results of Wahl et al. [19] for the same type of disc and operating under same conditions as mentioned in Table IV.

The comparison of present theoretical study and experimental results of Wahl et al. [19] for strain rates versus radial distance is shown graphically in Fig. 2. This graph depicts that there is a good agreement between the present theoretical and Wahl's experimental results for radial strain rates versus radial distance. The tangential strain rates also follow the same trend for present as well as experimental results of Wahl throughout the radial distance as one moves from inner to outer radii. A good agreement and similar

trends observed between the present theoretical and the Wahl's experimental strain rates inspires the confidence in the computer program developed.

III. Results and Discussion

A. Radial and Tangential Stresses

The effect of imposing thermal gradation on the creep behavior of the FGM disc is discussed here by determining the stress distributions.

Fig. 3 shows the variation of radial stress along radial distance in the rotating discs D_1, D_2, D_3 and D_4. As one moves radially outwards from inner radius, the radial stresses increases from zero, reaches a maximum value near middle of the disc and then decreases to zero towards the outer radius. Disc operating at linear thermal gradient shows more radial stress as compared to disc operating at uniform temperature throughout the radial distance. The maximum value of radial stress for discs D_4, D_3, D_2 and D_1 are $35.24MPa$, $35.08MPa$, $34.92MPa$ and $34.77MPa$, respectively, near the middle of the disc at radius $0.08001m$.

The variation of tangential stresses along radial distance under the effect of thermal gradation is shown graphically in Fig. 4. The graph shows that the tangential stresses increase from the inner radius, attain maximum values of $81.66MPa$, $81.34MPa$, $81.01MPa$ and $80.69MPa$ at radius $0.0619m$ for discs D_4, D_3, D_2 and D_1 respectively, and then decreases to $65.84MPa$ as one approaches outer radius. The tangential stress is highest for disc having maximum linear thermal gradation and disc having uniform temperature distribution has lowest tangential stress along the radial distance.

B. Strain Rates

The effect of imposing various linear thermal gradations on the creep behavior of the FGM disc is discussed here by determining the strain rate distributions. Fig. 5 shows graphically the effect of thermal gradations on radial strain rates along radial distance developed in rotating discs D_1, D_2, D_3 and D_4. The radial strain rates are compressive in nature throughout the radial distance. At the inner radius, disc D_4 shows the highest strain rate i.e. $1.34\times10^{-6}s^{-1}$ whereas disc D_1 shows the lowest strain rate i.e. $7.74\times10^{-8}s^{-1}$. The figure shows that the strain rate decreases as one move towards the outer radius. Now, disc D_4 attains the lowest strain rate of $1.08\times10^{-8}s^{-1}$ and disc D_1 attains the highest strain rate of $1.92\times10^{-9}s^{-1}$. Thus it is clear from the results that as the thermal gradation increases the strain rate decreases along the radial distance.

The variation of tangential strain rates along radial distance for discs D_1, D_2, D_3 and D_4 under the effect of thermal gradation is shown in Fig. 6. At the inner radius, disc D_1 has lowest tangential strain rate $1.54\times10^{-7}s^{-1}$ and disc D_4 has highest strain rate $2.68\times10^{-6}s^{-1}$. At the outer radius, disc D_1 has highest tangential strain rate $2.17\times10^{-8}s^{-1}$ and disc D_4 has lowest strain rate of $3.84\times10^{-9}s^{-1}$. The graph clearly shows that the tangential strain rate decreases for the discs along the radial distance as the thermal gradation increases.

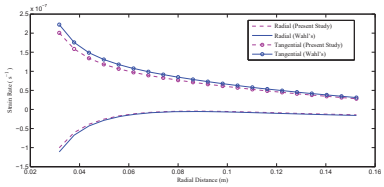

Fig. 2 Present theoretical results vs experimental results of Wahl et al. [19]

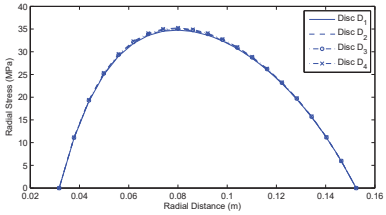

Fig. 3 Variation of radial stress along radial distance in discs D_1, D_2, D_3 and D_4 operating under thermal gradient

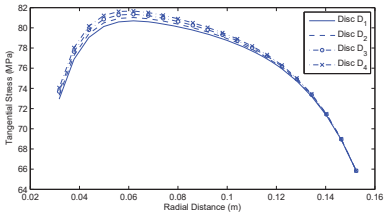

Fig. 4 Variation of tangential stress along radial distance in discs D_1, D_2, D_3 and D_4 operating under thermal gradient

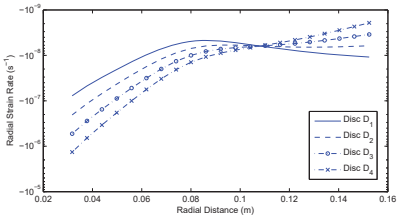

Fig. 5 Variation of radial strain rate along radial distance in discs D_1, D_2, D_3 and D_4 operating under thermal gradient

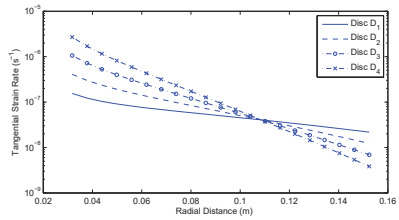

Fig. 6 Variation of tangential strain rate along radial distance in discs D_1, D_2, D_3 and D_4 operating under thermal gradient

IV. Conclusion

The present study reveals that as the thermal gradation increases, there is marginal change in the radial stress along radial distance. The radial stress traces a parabolic path as one moves from the inner radius towards the outer radius. The tangential stress developed in the rotating FGM disc increases near the inner radius and then decreases as one moves toward the outer radius. When the temperature decreases linearly from inner to outer radius, the radial strain rate decreases as one moves from the inner radius and then increases at the outer radius. At the inner radius, the disc with maximum thermal gradient shows the highest radial strain rate whereas at the outer radius, the same disc shows the lowest strain rate. The radial strain rate is compressive in nature throughout the disc. At the inner radius, the tangential strain rate developed in thermally graded rotating disc increases in comparison to disc operating at uniform temperature whereas, strain rate shows opposite trend at the outer radius. Thus, the graph makes it clear, when the disc is rotating under linearly decreasing temperature profile, the steady-state creep rate is minimum as compared to the disc rotating at uniform temperature. Therefore extension of the domain of thermal gradation to the design of rotating discs will be beneficial for material engineers and designers.

References

[1] S. F. Ahmadi and M. Eskandari, *Rocking rotation of a rigid disk embedded in a transversely isotropic half-space*. Civil Engineering Infrastructures Journal, 47(1), 125-138, 2014.

[2] S. M. Arnold, A. F. Saleeb and N. R. Al-Zoubi, *Deformation and life analysis of composite flywheel disk and multi-disk systems*. NASA/TM-2001-210578, 1-50, 2001.

[3] V. Birman and L. W. Byrd, *Modeling and analysis of functionally graded materials and structures*. Applied Mechanics Reviews, 60, 195-216, 2007.

[4] T. W. Clyne and P. J. Withers, *An introduction to metal matrix composites*. Cambridge University Press, Cambridge, 479, 1993.

[5] J. F. Durodola and O. Attia, *Deformation and stresses in functionally graded rotating disks*. Composites Science and Technology, 60, 987-995, 1999.

[6] M. Garg, B. S. Salaria and V. K. Gupta, *Effect of thermal gradient on steady state creep in a rotating disc of variable thickness*. Procedia Engineering 55, 542-547, 2013.

[7] V. K. Gupta, S. B. Singh, H. N. Chandrawat and S. Ray, *Creep behavior of a rotating functionally Graded composite disc operating under thermal gradient*. Metallurgical and Materials Transactions A, 35A, 1381-1391, 2004.

[8] V. K. Gupta, S. B. Singh, H. N. Chandrawat and S. Ray, *Steady state creep and material parameters in a rotating disc of* $Al-SiC_p$. European Journal of Mechanics A/Solids, 23, 335-344, 2004.

[9] T. Hirai and L. Chen, *Recent and prospective development of functionally graded materials in Japan*. Material Science Forum, 308-311, 509-514, 1999.

[10] *Metals Handbook(Vol. 2)*. American Society of Metals, 9th Ed., Metals Park, Ohio, USA, 714, 1978.

[11] A. B. Pandey, R. S. Mishra and Y. R. Mahajan, *Steady state creep behavior of silicon carbide particulate reinforced aluminum composites*. Acta Metall. Mater., 40(8), 2045-2052, 1992.

[12] K. T. Park, E. J. Lavernia and F. A. Mohamed, *High temperature creep of silicon carbide particulate reinforced aluminium*. Acta Metall. Mater., 38(11), 2149-2159, 1990.

[13] M. Rattan, S. B. Singh and S. Ray, *Effect of stress exponent on steady state creep in an isotropic rotating disc*. Bullitin of Calcutta Mathematical Society, 101(6), 559-570, 2009.

[14] M. Rattan, N. Chamoli and S. B. Singh, *Creep analysis of an isotropic functionally graded rotating disc*. International Journal of Contemporary Mathematical Sciences, 5(9), 419-431, 2010.

[15] O. D. Sherby, R. H. Klundt and A. K. Miller, *Flow stress, subgrain size and subgrain stability at elevated temperature*. Metall. Trans. A., 8, 843-850, 1977.

[16] T. Singh and V. K. Gupta, *Analysis of steady state creep in whisker reinforced functionally graded thick cylinder subjected to internal pressure by considering residual rtress*. Mechanics of Advanced Materials and Structures, 21, 384-392, 2014.

[17] K. Suryanarayanan, S. Praveen and S. Raghuraman, *Silicon carbide reinforced aluminium matrix composites for aerospace applications: A literature Review*. International Journal of Innovative Research in Science, Engineering and Technology, 2(11), 6336-6344, 2013.

[18] S. Uemura, *The activities of FGM on new application*. Material Science Forum, 423-425, 1-10, 2003.

[19] A. M. Wahl, G. O. Sankey, M. J. Manjoine, and E. Shoemaker, *Creep tests of rotating disks at elevated temperature and comparison with theory*. Journal Applied Mechanics, 76, 225-235, 1954.